Interference Mitigation via Cross-Tier Cooperation in Heterogeneous Cloud Radio Access Networks

Yujie Tang, *Member, IEEE*, Peng Yang, *Member, IEEE*, Wen Wu, *Student Member, IEEE*, Jon W. Mark, *Life Fellow, IEEE*, and Xuemin Shen, *Fellow, IEEE*

***Abstract*—In this paper, a cross-tier cooperation framework in H-CRAN is proposed to mitigate inter-tier interference. Specifically, a small cell remote radio head (S-RRH) acts as the relay for multiple macrocell users (MUEs), and obtains a fraction of time slot from multiple MUEs as a reward. Through the cooperation, the S-RRHs can obtain extra spectrum resource for serving small cell users (SUEs) which are secondary users, while the MUEs which are primary users can improve their data transmission utility. The cooperation problem is formulated as a mixed integer programming, which is NP-hard. To solve this problem, we transform the cooperation problem into a joint cooperation time and power allocation problem and a cooperator selection problem. First, we solve the joint cooperation time and power allocation problem to obtain the maximum cooperation utility of all the possible cooperating pairs. We derive the closed-form solution for the allocation problem by using linear independence constraint qualification and Karush-Kuhn-Tucker conditions. Then, we solve the cooperator selection problem by a two-sided matching algorithm. Extensive simulation results show that the utility of macrocell networks and small cell networks can be improved by adopting the proposed cooperation framework, and the cooperator selection result is stable and close-to-optimal.**

***Index Terms*—Heterogeneous cloud radio access network, cognitive radio, cooperation, interference mitigation, many-to-one matching.**

I. Introduction

THE EMERGING data-hungry mobile applications (e.g., mobile virtual reality, HD video streaming) will consume substantial spectrum resources in order to deliver satisfied quality of service (QoS) [2]. Meanwhile, mobile users' demands for ubiquitous wireless connections, gigabit per-user data rate, ultra-low end-to-end latency, and reduced communication costs are ever increasing. To meet these requirements, the heterogeneous cloud radio access network (H-CRAN) architecture, which integrates heterogeneous networks (HetNets) and cloud radio access networks (C-RANs), has been proposed to further improve both spectrum and energy efficiency, as well as network performance, through interference mitigation and dynamic spectrum sharing [3].

H-CRAN inherits the hierarchical architecture of HetNets to increase spectrum reuse, while the merits of C-RANs enable controlling the networks in a centralized manner at lower expenditure. In C-RANs, a large number of low-cost remote radio heads (RRHs), which are connected to the base band unit (BBU) pool, are widely deployed [4]. The resource allocation and interference management decisions are carried out at the BBU pool where cooperative processing schemes can be leveraged based on the cloud capabilities. In this way, C-RANs and HetNets are complementary in interference mitigation and resource allocation, which contribute to higher spectrum and energy efficiency. Moreover, the RRHs are connected to the BBU pool through high bandwidth fronthaul links, e.g., optical fiber and millimeter wave communications, to enable centralized processing and collaborative transmission [5]. In addition, the global knowledge available at the BBU pool enables the C-RANs to timely assign radio resources to RHHs according to the changes in user demand and mobility [6]. As a result, significant transmission rate improvement can be achieved due to reduced path-loss, joint scheduling, and signal processing. However, this new H-CRAN architecture introduces new challenges for novel resource allocation and performance optimization algorithms. Moreover, the characteristics of H-CRAN, including the network heterogeneity and high density, make the inference management a challenging task. Especially, the intra-tier interference among RRHs can be reduced with centralized cooperative processing in the BBU pool, while the inter-tier interference between small cell RRHs (S-RRHs) and the macrocell RRH (M-RRH) still needs to be addressed to fully unleash the potential of the H-CRAN architecture [7].

Aiming at reducing the inter-tier interference, cognitive radio (CR) can be leveraged by proactively avoiding co-channel interference, which results in higher spectrum and energy efficiency. Specifically, cognitive HetNets are capable of performing spectrum sensing, power and frequency adjustment [8]. In cognitive HetNets, the small cell base stations (SBSs) have to avoid being allocated with spectrum that is occupied by the macrocell networks. The key idea of inter-tier interference mitigation in cognitive HetNets is that, all small cell users (SUEs), which are secondary users, should autonomously sense the spectrum band of the macrocell and

Manuscript received May 15, 2019; revised October 19, 2019; accepted November 18, 2019. Date of publication December 4, 2019; date of current version March 6, 2020. This paper was accepted in part by IEEE ICC 2019 [1]. The associate editor coordinating the review of this article and approving it for publication was S. Zhou. *(Corresponding author: Peng Yang.)*

Y. Tang was with the Department of Electrical and Computer Engineering, University of Waterloo, Waterloo, ON N2L 3G1, Canada. She is now with the Department of Computer Science and Mathematics, Algoma University, Sault Ste. Marie, ON P6A 2G4, Canada (e-mail: yujie.tang@algomau.ca).

P. Yang, W. Wu, J. W. Mark, and X. Shen are with the Department of Electrical and Computer Engineering, University of Waterloo, Waterloo, ON N2L 3G1, Canada (e-mail: p38yang@uwaterloo.ca; w77wu@uwaterloo.ca; jwmark@uwaterloo.ca; sshen@uwaterloo.ca).

Digital Object Identifier 10.1109/TCCN.2019.2957457

report the sensing results. Therefore, the SBSs periodically allocate subframes to SUEs to perform spectrum sensing. However, in this case, spectrum sensing may not be accurate due to sensing errors (i.e., false alarm and miss detection) [9], and spectrum handover is required for the SUEs when the macrocell users (MUEs) reappear. SUEs may need to either switch to another temporarily idle channel or wait until the original channel is available again. As a result, it is important to explore the cooperation framework between the macrocell networks and the small cell networks. The resource allocation problem in the integrated architecture is challenging since it involves two parties that need to negotiate with the allocation decision.

Moreover, cooperator selection is also challenging since partner selection strategy affects the cooperation performance, i.e., the cooperator with better relay capability contributes to higher transmission rate. Hence, S-RRHs are chosen to act as the cooperators since they have more powerful relay capability than the SUEs, and they can support concurrent transmission as well. Thanks to the merits of C-RANs, the cooperator selection can be performed in a centralized manner with timely decision. To this end, we design a framework for cooperation between one or multiple MUEs and one S-RRH, and the benefit is quantified in terms of data transmission utility. The MUEs, who suffer from poor channel conditions, are allowed to access an S-RRH after the cooperation relationship between the S-RRH and the MUEs is established, and the S-RRH acts as a relay for these MUEs. In return, the cooperative S-RRH acquires a fraction of spectrum for serving SUEs as a reward. By cooperating with more MUEs, the S-RRHs will access more spectrum. More specifically, this cooperation framework can benefit the scenario in which the MUE is located at the cell edge and suffers from poor performance from the serving M-RRH. In this paper, to address the above challenges, we propose a cooperation framework to mitigate interference in the H-CRAN architecture, and the main contributions are summarized as follows.

- We establish the cooperation framework in the H-CRAN architecture with the objective of maximizing the data transmission utility and enhancing spectrum efficiency. The S-RRH acts as relay for MUEs while the SUEs adaptively tune their transmission power.
- We model the cooperation problem as a mixed integer programming, which is NP-hard. Then, the problem is transformed into a joint cooperation time and transmission power allocation problem and a cooperator selection problem. We derive the closed-form solution to the allocation problem by using linear independence constraint qualification (LICQ) and Karush-Kuhn-Tucker (KKT) conditions, while the cooperator selection problem is solved by a two-sided stable matching algorithm.
- We demonstrate the effectiveness of the proposed algorithm in improving data transmission utility via extensive simulations. In particular, MUEs can obtain higher data transmission utility, while S-RRHs can acquire more spectrum access opportunities for data transmission by serving SUEs. The inter-tier interference can be mitigated through cooperation as well.

The remainder of this paper is organized as follows. Section II reviews the related work. The system model is described in Section III. In Section IV, the cooperation problem in H-CRAN is formulated, followed by the proposed cooperator selection strategy in Section V. Numerical results are shown in Section VI. Finally, concluding remarks are given in Section VII.

II. Related Work

Extensive research efforts have been devoted to interference mitigation in HetNets [10]–[15]. In [11], Adhikary *et al.* investigated interference mitigation with massive-MIMO in HetNets where three interference coordination strategies with low complexity are proposed. The authors in [12] addressed the co-channel control and interference mitigation problem using directional antennas by establishing a stochastic geometry model. In [13], Li *et al.* studied the inter-tier interference coordination for HetNets where a 3D beamforming transmission approach is used for MUEs. Vu *et al.* formulated a joint load balancing and interference mitigation problem in HetNets as a network utility maximization problem to improve the cell-edge performance in [14]. In [15], a resource management approach is proposed that effectively manages interference across femtocells in a distributed manner.

Moreover, some research works investigate on interference mitigation for HetNets by using CR technology [16]–[20]. However, those works focus on interference mitigation for HetNets. Reducing interference is even more challenging for H-CRAN since interference mitigation is complicated with additional BBU pool in the network. Meanwhile, several cooperation frameworks have been investigated in various network scenarios to mitigate interference, such as in small cell networks and cognitive radio networks. In [21], an SU acts as a relay for an MUE. In return, the cooperative MUE grants a fraction of its superframe to the SU, and the cooperation is formulated as a coalitional game. In [22], Urgaonkar and Neely investigated a control scheme for cooperation between SUEs and MUEs under both cooperative relay model and interference model. Zhang *et al.* [23] investigated a cooperation scheme that multiple secondary users are coordinated to cooperatively sense the channels owned by the primary users for different interests. A subchannel allocation problem is formulated as a cooperative game among FUEs under the hybrid overlay/underlay access mode in [24]. In [25], a quadrature signaling based cooperation scheme is proposed to reduce the interference between primary users and secondary users in cognitive radio networks. In [26], Langar *et al.* proposed a game-theoretic scheme for strategic resource and power allocation problem in cooperative femtocell networks with a high density of femtocell access points, and they formulated the problem as an operations research game. Wu *et al.* [27] investigated the cooperative traffic offloading among mobile devices which are interested in receiving common contents from a cellular base station. The aforementioned works focus on interference mitigation in HetNets or CR networks.

In contrast, our work investigates the interference issue in the H-CRAN, which is more challenging. In an H-CRAN architecture, the infrastructures are different from the ones in HetNets or CRNs, whereas the conventional base stations are divided into BBUs and RRHs. Therefore, the coordination among RRHs as well as the coordination between RRHs and BBUs need to be investigated. In order to deal with these coordination issues, new models and schemes are required. Peng *et al.* [3] proposed a contract-based interference coordination scheme for downlink transmissions in H-CRAN. However, the baseband signal processing functionality is deployed in both the macro base station and the BBU pool, which compromises the benefits of separated base station functions in C-RANs. Moreover, interference management in uplink transmissions is more challenging since all users can independently adjust their transmission powers. Hence, the transmission rates of all users will be different from one to another accordingly. Therefore, we focus on a cooperation framework to mitigate interference for uplink transmissions. We consider the cooperation among multiple S-RRHs and MUEs. Compared to our prior work [1], we have extended it by allocating the cooperation time and transmission powers of the S-RRHs simultaneously to improve the system performance. The joint time and power allocation problem is difficult to solve since the objective function is non-convex. We solve the problem by using LICQ and KKT conditions. Moreover, we have illustrated the utility of the MUEs and S-RRHs via additional simulation results to demonstrate the effectiveness of the proposed algorithm.

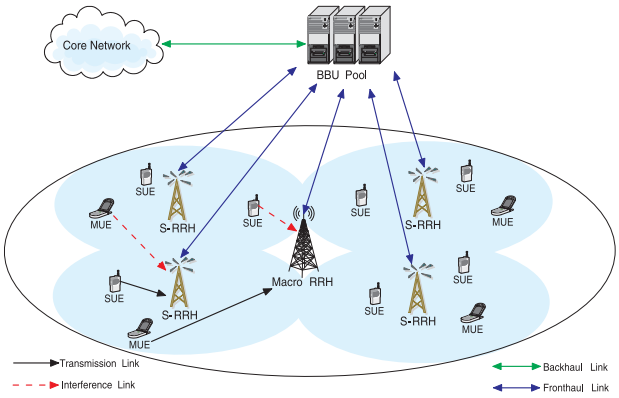

(a) Without cooperation. The black solid lines and red dash lines represent the transmission links and interference links, respectively.

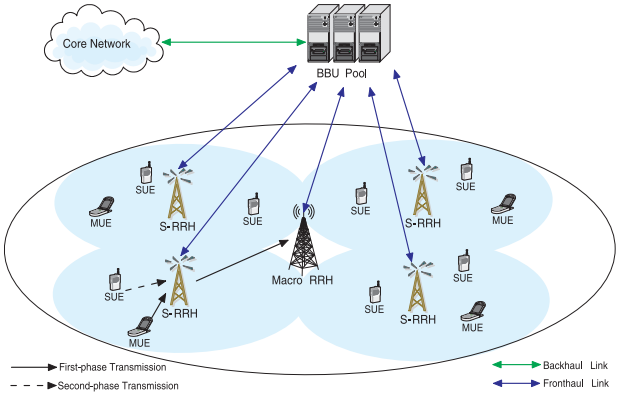

(b) With cooperation. The black solid lines and black dash lines represent the first-phase transmission and the second-phase transmission during the cooperation, respectively.

Fig. 1. The H-CRAN framework. The green link is the backhaul link between core network and BBU pool, and the blue links are the fronthaul links between BBU pool and RRHs.

III. System Model

A. Network Model

We consider the uplink transmissions of an orthogonal frequency division multiple access (OFDMA) H-CRAN system that consists of one M-RRH and multiple S-RRHs. The surrounding SUEs are served with probabilistic spectrum access opportunities. All the RRHs, including the M-RRH and the S-RRHs, are connected to the BBU pool via optical fibers or mmWave communications [28], as illustrated in Fig. 1. The small cell networks coexist with the macrocell networks. CR technology is adopted where each small cell base station senses the spectrum occupation of neighboring cells, and then accesses the spectrum via one of the disjoint subchannels, thus avoiding interference from adjacent small cells. Thanks to the centralized architecture of H-CRAN, the coordination among the small cell base stations can be implemented in the BBU pool to reduce the interference. We consider a single macrocell system in which $\mathcal{M} = \{1, 2, \ldots, M\}$ denotes the set of MUEs within the macrocell coverage and $\mathcal{K} = \{1, 2, \ldots, K\}$ denotes the set of S-RRHs. Each S-RRH serves a set of SUEs in its proximity, represented by set $\mathcal{N}_k$. Accordingly, each macrocell has K sets of SUEs $\mathcal{N} = \{\mathcal{N}_1, \mathcal{N}_2, \ldots, \mathcal{N}_K\}$, and $\mathcal{N}_k = \{1, 2, \ldots, |\mathcal{N}_k|\}$ where $|\mathcal{N}_k|$ represents the cardinality of set $\mathcal{N}_k$.

The spectrum access modes in HetNets can be classified into three types: open access, closed access and hybrid access [29]. In the open access mode, all the users of a cellular provider are allowed to access the S-RRH, such as the hotspot in a restaurant or shopping mall. However, the disadvantage of open access is the throughput of small cells decreases with the increasing number of users, and certain security issues remain to be addressed. According to a survey in [30], users prefer small cells with closed access mode, in which the S-RRH allows only its own subscribed users to establish connections. Most small cells deployed in residential areas employ this access mechanism for security reasons. Hence, we investigate a cooperation framework based on closed access mode in this work. MUEs are granted to communicate with the S-RRH after the cooperation relationship between MUEs and S-RRH has been established.

B. UE Utility Model

The cooperation between MUEs and S-RRHs operates in a time-slotted manner. The channels are considered to be stable during a fixed time slot T, but vary independently from one slot to another. The assumption that the channel state information (CSI) is available is commonly used, and note that in practical H-CRAN, CSI needs to be obtained via various estimation

techniques including the minimum mean-square-error estimation, the least squares estimation, and the maximum-likelihood estimation [31], which is, however, out of the scope of this work. Instead, a time slotted system is adopted. In each time slot *T*, we model the wireless channel as a distance-based log-normal distributed shadowing channel [32]. The channel gain is given by

$$h^2 = Sd^{-\gamma}|g|^2 \tag{1}$$

where $\gamma \in [3, 5]$ is the path loss exponent [33], and d denotes the distance between the transmitter and receiver. S is the log-normal shadow fading variable with mean of 0 dB and standard deviation of δ_S dB, and $|g|$ is the Rayleigh fading magnitude with $\mathbb{E}[|g|^2] = 1$.

1) Non-Cooperation Mode: In the non-cooperation mode, the utility of transmission from MUE_m ($m \in \mathcal{M}$) to the M-RRH can be written as:

$$U_m = TB_m \log_2\left(1 + \frac{h_{m,0}^2 P_m}{\sum_{n\in\Omega_m} h_{n,0}^2 P_n + \sigma^2}\right) \tag{2}$$

where B_m is the bandwidth, and T represents the duration of one time slot. P_m is the transmission power of MUE_m, and P_n is the transmission power of SUE_n. The channel fading coefficients from MUE_m to the M-RRH and from SUE_n to the M-RRH are denoted by $h_{m,0}$ and $h_{n,0}$, respectively. $n \in \Omega_m$ is the set of SUEs operating on the same subchannel with MUE_m, and σ^2 is the variance of the additive white Gaussian noise.

In the closed access mode, any unregistered users approaching the S-RRH will experience adverse interference. The utility of SUE_n ($n \in \mathcal{N}_k$) transmitting to the $\mathrm{S\text{-}RRH}_k$ ($k \in \mathcal{K}$) is calculated by

$$U_n^k = TB_n^k \log_2\left(1 + \frac{h_{n,k}^2 P_n}{\sum_{m\in\Psi_n} h_{m,k}^2 P_m + \sigma^2}\right) \tag{3}$$

where $h_{n,k}$ and $h_{m,k}$ represent the channel fading coefficients from SUE_n to $\mathrm{S\text{-}RRH}_k$ and from MUE_m to $\mathrm{S\text{-}RRH}_k$, respectively. B_n^k denotes the bandwidth allocated to SUE_n served by $\mathrm{S\text{-}RRH}_k$. $m \in \Psi_n$ is the set of MUEs operating on the same subchannel with SUE_n.

The outage probability of MUE and SUE can be computed as the probability of the signal to interference plus noise ratio (SINR) below a certain threshold θ_m and θ_n, and are given by

$$P_{out_m} = P_r\left\{\frac{h_{m,0}^2 P_m}{\sum_{n\in\Omega_m} h_{n,0}^2 P_n + \sigma^2} \le \theta_m\right\}, \tag{4}$$

$$P_{out_n} = P_r\left\{\frac{h_{n,k}^2 P_n}{\sum_{m\in\Psi_n} h_{m,k}^2 P_m + \sigma^2} \le \theta_n\right\}. \tag{5}$$

We present the utility equations of non-cooperation mode to illustrate the difference compared with the cooperation mode, which is given in the following subsection.

2) Cooperation Mode: Cooperation can help improve the utility of macrocell network and small cell network simultaneously. MUEs transmit data to the S-RRHs, and then the S-RRHs relay MUEs' data to the M-RRH. Therefore, in the cooperation mode, the utility of MUE_m cooperating with $\mathrm{S\text{-}RRH}_k$ is expressed as (see (12) and (13) in [34])

$$\begin{aligned}\widetilde{U}_m^k &= \alpha_{k,m} TB_m \log_2\left(1 + \frac{SNR_{m,k}\cdot SNR_{k,0}}{SNR_{m,k} + SNR_{k,0} + 1}\right) \\ &= \alpha_{k,m} TB_m \log_2\left(1 + \frac{1}{\sigma^2}\cdot\frac{h_{m,k}^2 h_{k,0}^2 P_m P_k}{h_{m,k}^2 P_m + h_{k,0}^2 P_k + \sigma^2}\right)\end{aligned} \tag{6}$$

where $SNR_{m,k}$ and $SNR_{k,0}$ represent the signal-to-noise ratio from MUE_m to the $\mathrm{S\text{-}RRH}_k$ and from $\mathrm{S\text{-}RRH}_k$ to the M-RRH, respectively. P_k is the transmission power of $\mathrm{S\text{-}RRH}_k$, and $\alpha_{k,m}$ is a time fraction factor of $\mathrm{S\text{-}RRH}_k$ cooperating with MUE_m. $h_{m,k}$ and $h_{k,0}$ denote the channel fading coefficients from MUE_m to $\mathrm{S\text{-}RRH}_k$ and from $\mathrm{S\text{-}RRH}_k$ to M-RRH, respectively. Note that (6) is derived by multiplying the cooperation transmission rate and the cooperation time $\alpha_{k,m}$ on frequency band B_m, which represents the cooperation utility.

Similarly, the utility of SUE_n associated with $\mathrm{S\text{-}RRH}_k$ gained through cooperation with the MUE_m is given by

$$\widetilde{U}_n^k = \left(1 - \alpha_{k,m}\right) T\widetilde{B}_n^k \log_2\left(1 + \frac{h_{n,k}^2 P_n}{\sigma^2}\right) \tag{7}$$

where $\widetilde{B}_n^k = \frac{B_m q_k}{|\mathcal{N}_k|}$. $|\mathcal{N}_k|$ is the number of SUEs which are served by $\mathrm{S\text{-}RRH}_k$, and q_k is the number of MUEs that $\mathrm{S\text{-}RRH}_k$ cooperates with. It is worth noting that, for (6) and (7), they are formulated based on SNR as interference does not exist due to cooperation. Since the S-RRHs choose to cooperate with the MUEs, the SUEs who are served by the S-RRHs will not cause the interference to the MUEs.

IV. Problem Formulation

The small cell networks are formed based on the spectrum requirements from geographically close SUEs. The S-RRHs cooperate with the MUEs who suffer from poor throughput performance. The S-RRHs operate as relays to help MUEs transmit data since the S-RRHs have better relaying capability than that of the SUEs. In return, the S-RRHs acquire extra spectrum access opportunities for serving SUEs. The cooperation between MUEs and S-RRHs is a win-win game in that the MUEs can improve their performance, and the S-RRHs can help SUEs acquire more spectrum resource.

When the BBU pool performs resource allocation, cooperation formulation is also considered. During the cooperation process, $\mathrm{S\text{-}RRH}_k$ cooperates with multiple MUEs within interval $\alpha_{k,m}\,T$. In return, the $\mathrm{S\text{-}RRH}_k$ acquires the remaining time slot $(1-\alpha_{k,m})\,T$ for its serving SUEs. Note that different S-RRHs have distinct $\alpha_{k,m}$. Therefore, the optimization problem of our proposed cooperation framework can be formulated as follows:

$$\begin{aligned}(\mathcal{P}):\ &\underset{x_{k,m},\alpha_{k,m},P_k}{\text{maximize}} \sum_{k\in\mathcal{K}}\sum_{m\in\mathcal{M}} x_{k,m}\left(\widetilde{U}_m^k + \sum_{n\in\mathcal{N}_k}\widetilde{U}_n^k\right) \\ &\text{subject to } \sum_{k\in\mathcal{K}} x_{k,m} \le 1,\ \forall m \in \mathcal{M}\end{aligned}$$

$$\begin{aligned}
&\sum_{m\in\mathcal{M}} x_{k,m} \le q_k,\ \forall k \in \mathcal{K} \\
&x_{k,m} \in \{0,1\},\ \forall k \in \mathcal{K}, m \in \mathcal{M} \\
&0 \le \alpha_{k,m} \le 1,\ \forall k \in \mathcal{K}, m \in \mathcal{M} \\
&P_{min} \le P_k \le P_{max} \\
&\widetilde{U}_m^k \ge U_m^{min},\ \forall k \in \mathcal{K} \\
&\sum_{n\in\mathcal{N}_k} \widetilde{U}_n^k \ge U_k^{min},\ \forall m \in \mathcal{M} \qquad (8)
\end{aligned}$$

where $\widetilde{U}_m^k$ and $\widetilde{U}_n^k$ are given by (6) and (7), respectively. $x_{k,m} = 1$ indicates that S-RRH$_k$ is assigned to cooperate with MUE$_m$. Otherwise, $x_{k,m} = 0$. The first constraint indicates that MUE$_m$ can be associated with at most one S-RRH. q_k is the maximum number of MUEs the S-RRH$_k$ choose to cooperate with. The second constraint means that each S-RRH$_k$ can cooperate with at most q_k MUEs. P_{min} and P_{max} are the minimum and maximum transmission power of S-RRH$_k$, respectively. U_m^{min} and U_k^{min} denote the minimum achieved cooperation utility for the MUEs and S-RRHs, respectively.

The optimization problem (8) is a mixed integer optimization problem which is NP-hard. There is no readily available algorithm that gives the optimal solution to NP-hard problems at large scale within a reasonable amount of computational effort and time. To solve this problem, we transform it into a joint cooperation time and transmission power allocation problem and a many-to-one matching problem [35], [36]. The optimal solutions of $\alpha_{k,m}$ and P_k are firstly obtained by the BBU pool and broadcasted to the RRHs and users. Then, the MUEs, of which transmission condition is poor, join the cooperation to improve their performance. The S-RRHs that require spectrum access opportunities also join a stable matching set with MUEs. Afterwards, the S-RRHs and MUEs generate their cooperating preference lists separately. Then, by adopting the two-sided cooperator selection algorithm, matched cooperation pairs between one S-RRH and multiple MUEs can be obtained.

In the following, we focus on tackling problem $\mathcal{P}$ to obtain the optimal solution on joint cooperation time and power allocation and cooperator selection which correspond to the three variables α_k, P_k and $x_{k,m}$ in the objective function. The value of $x_{k,m}$ depends on the values of $\alpha_{k,m}$ and P_k since they contribute to the positions in the MUEs preference lists. But the values of $\alpha_{k,m}$ and P_k are not affected by $x_{k,m}$. Therefore, to tackle the challenging problem $\mathcal{P}$, we take full use of its special structure and further decompose it into an equivalent cooperation time and power allocation problem $\mathcal{P}_1$ and cooperator selection problem $\mathcal{P}_2$, respectively.

A. Cooperation Time and Power Allocation Problem

As mentioned above, we need to obtain the values of $\alpha_{k,m}$ and P_k for each S-RRH first. However, how to choose the values of $\alpha_{k,m}$ and P_k for each S-RRH is challenging. On one hand, the MUEs are expecting an $\alpha_{k,m}$ value to be as large as possible to increase their utility; on the other hand, the S-RRHs prefer a smaller value of $\alpha_{k,m}$, since smaller $\alpha_{k,m}$ gives longer spectrum access time for their serving SUEs. This contradiction seems to be hard to deal with, but we notice that when the MUEs have the minimum cooperation utility requirement, the value of $\alpha_{k,m}$ can be compensated with the increasing value of P_k. Hence, we take the total utility of the cooperation pair between MUE and S-RRH into consideration, which is shown in $\mathcal{P}_1$

$$\begin{aligned}
(\mathcal{P}_1): \underset{\alpha_{k,m},P_k}{\text{maximize}}\ & \widetilde{U}_m^k + \sum_{n\in\mathcal{N}_k} \widetilde{U}_n^k \\
\text{subject to}\ & 0 \le \alpha_{k,m} \le 1,\ \forall k \in \mathcal{K}, m \in \mathcal{M} \\
& P_{min} \le P_k \le P_{max} \\
& \widetilde{U}_m^k \ge U_m^{min},\ \forall k \in \mathcal{K} \\
& v \sum_{n\in\mathcal{N}_k} \widetilde{U}_n^k \ge U_k^{min},\ \forall m \in \mathcal{M}. \qquad (9)
\end{aligned}$$

The optimal values of $\alpha_{k,m}$ and P_k are decided based on channel conditions and the minimum cooperation utility requirement of S-RRHs and MUEs, which will be elaborated in Section V.

B. Cooperator Selection Problem

When the feasible solutions of $\alpha_{k,m}$ and P_k are obtained by solving $\mathcal{P}_1$, we can formulate a cooperator selection problem, denoted by

$$\begin{aligned}
(\mathcal{P}_2): \underset{x_{k,m}}{\text{maximize}}\ & \sum_{k\in\mathcal{K}} \sum_{m\in\mathcal{M}} x_{k,m} U_{k,m} \\
\text{subject to}\ & \sum_{k\in\mathcal{K}} x_{k,m} \le 1,\ \forall m \in \mathcal{M} \\
& \sum_{m\in\mathcal{M}} x_{k,m} \le q_k,\ \forall k \in \mathcal{K} \\
& x_{k,m} \in \{0,1\},\ \forall k \in \mathcal{K}, m \in \mathcal{M} \qquad (10)
\end{aligned}$$

where $U_{k,m} = \widetilde{U}_m^k + \sum_{n\in\mathcal{N}_k} \widetilde{U}_n^k$. We convert the cooperator selection problem into a many-to-one matching problem and solve it by the two-sided cooperator selection algorithm.

We decompose the primary optimization problem into two sub-problems: the cooperation time and power allocation problem and the cooperator selection problem. In the primary optimization problem, the two sub-problems are coupled with each other. The values of cooperation time fraction and transmission power depend on the cooperation pairs between S-RRHs and MUEs since different choices of the cooperator partners contribute to different data transmission utility, and vice versa. However, in the first sub-problem, we obtain the cooperation time fraction and transmission power of all the possible cooperation pairs, and then, choose the optimal one with the highest data transmission utility. The complexity of solving the problem is increased by using the decomposition method, but we can achieve the near optimal solution of the original NP-hard problem.

V. Cooperator Selection Strategy

In this section, we present the cooperation procedure. Then, we give the closed-form solution of problem $\mathcal{P}$ by solving cooperation time and power allocation problem $\mathcal{P}_1$ and cooperator selection problem $\mathcal{P}_2$, respectively. Particularly, problem $\mathcal{P}_1$ is addressed to achieve the optimal $\alpha_{k,m}$ and P_k by using

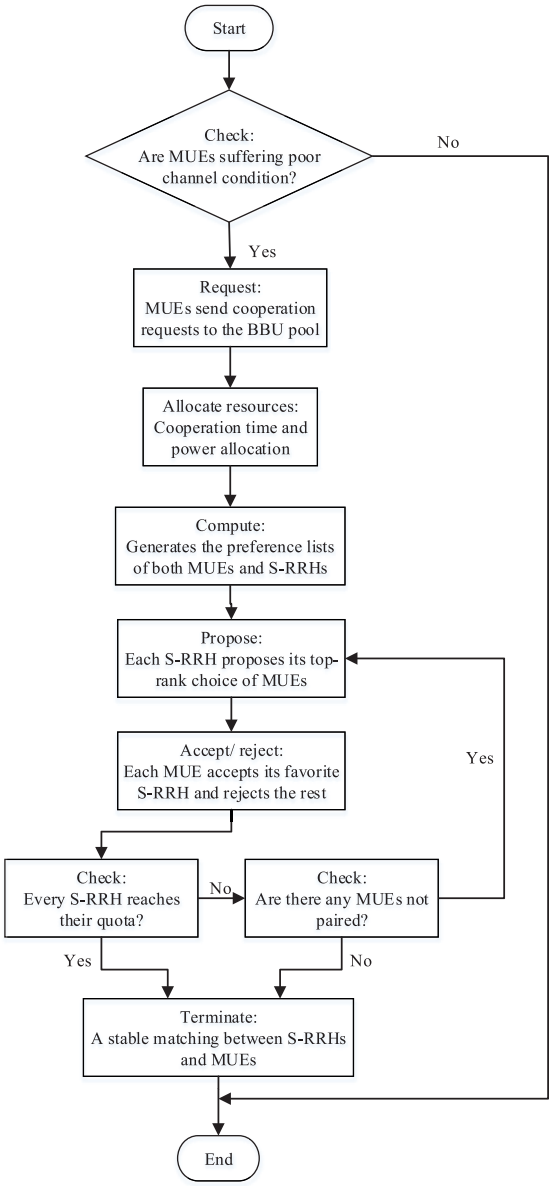

Fig. 2. Flow diagram of the cooperation procedure.

KKT conditions, and the optimal cooperator selection problem $\mathcal{P}_2$ is tackled to obtain the optimal cooperator selection from the viewpoint of bipartite graph many-to-one matching.

A. Cooperation Procedure

The proposed cooperation procedure is performed according to the flow chart in Fig. 2. When the transmission links of the MUEs are in poor condition, they will firstly send the cooperation requests to the nearby S-RRHs. Second, if the S-RRHs would like to accept the requests, they will send the feedback information together with their relaying power P_k and cooperation time fraction $\alpha_{k,m}$ to the MUEs. Third, both the MUEs and S-RRHs will generate their cooperation preference lists. Finally, a many-to-one stable matching is performed to establish the cooperation pairs.

B. Cooperation Time and Power Allocation Problem

From the objective function of problem $\mathcal{P}_1$, we can see that the first term of the function increases with $\alpha_{k,m}$ and P_k while the second term decreases with $\alpha_{k,m}$, without being effected by the P_k. Based on (6) and (7), we have

$$\begin{aligned} U_{k,m} &= \widetilde{U}_m^k + \sum_{n\in\mathcal{N}_k} \widetilde{U}_n^k \\ &= TB_m\big\{\big[F_{k,m}(P_k) - G_{k,m}\big]\alpha_{k,m} + G_{k,m}\big\}, \end{aligned} \tag{11}$$

where

$$F_{k,m}(P_k) = \log_2\left(1 + \frac{1}{\sigma^2}\cdot\frac{h_{m,k}^2 h_{k,0}^2 P_m P_k}{h_{m,k}^2 P_m + h_{k,0}^2 P_k + \sigma^2}\right) \tag{12}$$

and

$$G_{k,m} = \frac{q_k}{|\mathcal{N}_k|}\sum_{n\in\mathcal{N}_k}\log_2\left(1 + \frac{h_{n,k}^2 P_n}{\sum_{m\epsilon\Phi_n} h_{m,k}^2 P_m + \sigma^2}\right). \tag{13}$$

Therefore, we can rewrite the optimization problem $\mathcal{P}_1$ as

$$\begin{aligned} (\mathcal{P}_1'): \underset{\alpha_{k,m},P_k}{\text{minimize}} \quad & TB_m\big\{\big[G_{k,m} - F_{k,m}(P_k)\big]\alpha_{k,m} - G_{k,m}\big\} \\ \text{subject to} \quad & \alpha_{k,m} \geq 0 \\ & -\alpha_{k,m} + 1 \geq 0 \\ & P_k - P_{min} \geq 0 \\ & -P_k + P_{max} \geq 0 \\ & \alpha_{k,m} TB_m F_{k,m}(P_k) - U_m^{min} \geq 0 \\ & \big(1-\alpha_{k,m}\big) TB_m G_{k,m} - U_k^{min} \geq 0. \end{aligned} \tag{14}$$

It is difficult to obtain the closed-form solution of the above nonconvex problem, so it is preferable to linearize and solve the optimization problem in dual space, but the resultant computation is intensive. For our purpose, it is feasible to solve the problem as discussed below.

Using first-order necessary conditions, we are considering the following program. Since the objective function is continuous, we can rewrite the constraints as $0 \leq \alpha_{k,m} \leq 1$, $P_{min} \leq P_k \leq P_{max}$, $\alpha_{k,m} TB_m F_{k,m}(P_k) - U_m^{min} \geq 0$ and $\alpha_{k,m} \leq 1 - \frac{U_k^{min}}{TB_m G_{k,m}}$. Since $U_k^{min} \leq TB_m G_{k,m}$, the $1 - \frac{U_k^{min}}{TB_m G_{k,m}} \leq 1$. We can find that the feasible solution of $\mathcal{P}_1'$ is a closed set with $0 \leq \alpha_{k,m} \leq 1 - \frac{U_k^{min}}{TB_m G_{k,m}}$ and $P_{min} \leq P_k \leq P_{max}$.

Proposition 1: In problem $\mathcal{P}_1'$, there must be a feasible solution and the solution reaches the optimal point at the boundary.

Please refer to the Appendix for the proof of this proposition. Therefore, we can obtain the optimal solutions $\alpha^*_{k,m}$ and P^*_k as

$$\alpha^*_{k,m}\begin{cases} = 1 - \dfrac{|\mathcal{N}_k| U_k^{min}}{q_k TB_m \log_2\left(1+\frac{h^2_{n,k}P_n}{\sum_{m\epsilon\Phi_n} h^2_{m,k}P_m+\sigma^2}\right)}, \\ \quad G_{k,m} < F_{k,m}(P_{max}) \\ = \dfrac{U_m^{min}}{TB_m F_{k,m}(P_{max})}, \ G_{k,m} > F_{k,m}(P_{max}) \\ \quad \in \left[\dfrac{U_m^{min}}{TB_m F_{k,m}(P_{max})}, \ 1 - \dfrac{|\mathcal{N}_k| U_k^{min}}{q_k TB_m}\right. \\ \qquad \left. \times \dfrac{1}{\log_2\left(1+\frac{h^2_{n,k}P_n}{\sum_{m\epsilon\Phi_n} h^2_{m,k}P_m+\sigma^2}\right)}\right], \\ \quad G_{k,m} = F_{k,m}(P_{max}) \end{cases} \tag{15}$$

and

$$P^*_k = P_{max}. \tag{16}$$

There are three different optimal solutions of $\alpha_{k,m}$ depending on three different conditions, and the optimal solution of P_k is achieved at the maximum value. After problem $\mathcal{P}_1$ is solved, we will address $\mathcal{P}_2$ in the following.

C. Many-to-One Matching for Cooperator Selection Problem

In this subsection, we first convert the optimization problem $\mathcal{P}_2$ into a bipartite graph, in which a many-to-one matching is needed. Then, we solve the many-to-one matching by using a two-sided stable matching algorithm.

The cooperation selection problem is converted into a many-to-one matching in which the cooperation consists of two sets of agents: *K* S-RRHs and *M* MUEs. S-RRHs are denoted by $\mathcal{K} = \{1, 2, \ldots, K\}$, and MUEs are expressed by $\mathcal{M} = \{1, 2, \ldots, M\}$. In reality, each agent has a strict preference list of the acceptable agents on the other side. Let $\Gamma \subseteq \mathcal{K} \times \mathcal{M}$ denote the set of acceptable pairs. q_k is a positive integer which denotes the quota, in other words, it is allowed up to q_k MUEs cooperating with S-RRH *k*. Without loss of generality, we assume that (i) *k* finds *m* acceptable if and only if *m* finds *k* acceptable, and in this case, we say that (*k*, *m*) is an acceptable pair; (ii) S-RRH *k* finds at least q_k MUEs acceptable, and each MUE finds one S-RRH acceptable. Note that we consider the preference lists in which the S-RRHs have preferences over individual MUEs, not over groups of MUEs.

With the aim of not only trying to maximize the cooperation utility, but also considering the stability of the cooperation, we adopt the two-sided many-to-one stable matching approach which takes both parties' interests into consideration. Each user has a preference ranking list of acceptable users on the other side. Each user in set $\mathcal{K}$ (or $\mathcal{M}$) has preference over users in set $\mathcal{M}$ (or $\mathcal{K}$). Let $\psi(k)$ be the preference function of user *k* in set $\mathcal{K}$, and let $\varphi(m)$ be the preference function of user *m* in set $\mathcal{M}$. Hence, each S-RRH has a preference set $\psi(k)$ for MUEs, which is sorted according to $\sum_{n\in\mathcal{N}_k} \widetilde{U}^k_n$, i.e., the total utility $\mathrm{S\text{-}RRH}_k$ can acquire by cooperating with the MUE. Each MUE also has its own preference set $\varphi(m)$, which is ordered according to $\widetilde{U}^k_m$, the utility that MUE can obtain through cooperation with the S-RRH. In particular, $i \succ_k j$ iff S-RRH *k* prefers MUE *i* to MUE *j*. The incidence matrix $\mathcal{X}$ is a subset of μ and is defined by: $x_{k,m} = 1$, if $(k, m) \in \mu$, and $x_{k,m} = 0$ otherwise. The objective of the matching is to find a stable matching solution. It is evident that μ is a stable matching of (Γ, q_k) if and only if its incidence matrix *x* satisfies the following inequalities:

$$\sum_{k:(k,m)\in\Gamma} x_{k,m} \le 1, \ \forall m \in \mathcal{M} \tag{17}$$

$$\sum_{m:(k,m)\in\Gamma} x_{k,m} \le q_k, \ \forall k \in \mathcal{K} \tag{18}$$

$$q_k x_{k,m} + q_k \sum_{i\succ_m k} x_{i,m} + \sum_{j\succ_k m} x_{k,j} \ge q_k, \ \forall (k,m) \in \Gamma. \tag{19}$$

Indeed, the first two inequalities ensure that μ is a matching, and the last inequality guarantees that the matching is stable. Expression $i \succ_z j$ represents user *z* prefers *i* to *j*.

The two-sided cooperator selection algorithm is performed to solve the cooperation problem, and it can be summarized by the following steps in detail. In the first beginning, the data transmission utility of MUEs obtained by cooperating with S-RRHs are calculated to get the preference lists of S-RRHs of all MUEs, and the preferences are sorted in descending order. In addition, the S-RRHs have the privilege to choose the MUEs and form the preference lists based on the cooperation utility. Each S-RRH proposes to its top-ranked choice (if an S-RRH has a quota of q_k, then the q_k MUEs are the top-ranked on its ranking list). Afterwards, the MUE checks whether one of the proposals from the S-RRHs is its most preferred cooperator according to its preference ranking list. If no such matching is found, the algorithm proceeds to the next step, where the second ranked MUE on each S-RRH's ranking list is matched with the top-ranked MUEs on the S-RRH's list.

For example, there are 2 S-RRHs and 6 MUEs. Each of the S-RRHs and MUEs has its own preference lists, e.g., $\{S_1, S_2\}$ for the MUE_1 and $\{M_1, M_4, M_3, M_6, M_5, M_2\}$ for $\mathrm{S\text{-}RRH}_1$. $\mathrm{S\text{-}RRH}_1$ has quota 2 so that it will propose to the top two MUEs on its preference list, i.e., MUE_1 and MUE_4. If MUE_1 or MUE_4 accepts the proposal, the matching pairs will be updated; otherwise, it will continue to propose the one next on its reference list. In any step where no matching is found, the algorithm proceeds to the next step. Otherwise, the matched pairs are under the tentative-assignment-and-update state. Finally, when the pairs are under the tentative-assignment-and-update state from the ℓth step, the tentative matched pairs, i.e., S-RRHs and MUEs, are updated in the following way.

- Any S-RRH who ranks lower than the MUE's tentatively assigned cooperator is deleted from its ranking list, i.e., the updated ranking of the MUE who is tentatively assigned to its ℓth choice lists only its ℓth first choice;
- MUE is deleted from the ranking of any S-RRH who was deleted from the MUE's ranking list.

According to the above statement, the cooperator selection algorithm is sketched in Algorithm 1.

Algorithm 1 Two-Sided Cooperator Selection Algorithm

Input:

A set of S-RRHs $\mathcal{K}$, a set of MUEs $\mathcal{M}$, and preference ranking lists $\psi(k)$, $\varphi(m)$ of the S-RRHs and MUEs, respectively.

Initialize q_k, $\mu = \emptyset$ and $\ell = 0$;

Output:

The cooperation pairs selection, i.e., many-to-one matching result μ;

1: **while** (S-RRH *k* is not fully subscribed) and ($\psi(k) \neq \emptyset$) **do**
2: S-RRH *k* proposes to the MUEs who are the first $(q_k + \ell)$th choice in the preference ranking list $\psi(k)$.
3: **if** S-RRH *k* is the first choice in MUE *m*'s preference ranking list $\varphi(m)$ **then**
4: $q_k = q_k - 1$, $\mu = \mu \cup \{(k, m)\}$, and update the ranking lists $\psi(k)$, $\varphi(m)$ of the S-RRHs and MUEs, respectively;
5: **else**
6: $\ell = \ell + 1$, and go back to step 2;
7: **end if**
8: **end while**
9: μ is a stable matching.

Before we move forward to the part of proving the propositions of the two-sided cooperator selection algorithm, we need two theorems in advance which will help deduct the proofs.

Theorem 1: A pair $(k, m) \in \Gamma$ blocks μ if (i) *k* prefers *m* to at least one of its assigned MUEs in μ, or if *k* is assigned fewer than q_k MUEs, and (ii) *m* prefers *k* to its assigned S-RRH in μ, or if *m* is unmatched.

Theorem 2: A matching result μ is stable if it is not blocked by any pair of users.

Based on the Theorem 1 and Theorem 2, we have the following propositions.

Proposition 2: Stable matching can be obtained based on the two-sided cooperator selection algorithm.

Proof: We prove the proposition by contradiction. Let μ be the matching result acquired using the two-sided cooperator selection algorithm. Suppose (*k*, *m*) will block μ, i.e., S-RRH *k* and MUE *m* are not matched indicating that the pair (*k*, *m*) does not belong to μ, but they prefer each other more. Therefore, MUE *m* prefers S-RRH *k* more than other S-RRHs on its preference ranking list $\varphi(m)$, i.e., $k \succ_m \mu(m)$. Moreover, S-RRH *k* must have proposed to MUE *m* before the matching algorithm stops. However, they do not match each other in the matching result μ, which suggests that MUE *m* must reject the proposal of S-RRH *k*. In this case, there must be another S-RRH k' who has a higher priority in MUE *m*'s preference ranking list in μ. As a result, (*k*, *m*) will not block μ, which contradicts the assumption. Hence, matching result μ is a stable matching since it will not be blocked by any users. ■

Proposition 3: Stable matching for the two-sided cooperation pair selection problem is unique.

Proof: We prove the proposition by induction on *M*. Let *K* be the number of S-RRHs with quota q_k, *M* be the number of MUEs, and μ be the matching for matrix $\Gamma_{\mathcal{K}\times\mathcal{M}}$. When $M = 1$, the stable matching is unique since the first and the best MUEs will be assigned to the only S-RRH; when $M \geq 2$, let μ be the matching result which enables the S-RRHs choose the MUEs providing highest cooperation utility for Γ, and let μ' be the matching attained by deleting a S-RRH *k* and MUE *m* to attain Γ'. Suppose μ' is the unique stable matching for Γ'. If μ is a stable matching, then $\mu(k) = m$, and $\mu \backslash \{(k, m)\}$ must be a stable matching. By induction, we can conclude that $\mu := \mu' \cup \{(k, m)\}$ is the unique stable matching for Γ. Therefore, μ is the unique stable matching for Γ. ■

Proposition 4: The proposed two-sided cooperator matching scheme always converges to a stable matching.

Proof: To see that the scheme converges, note that each MUE can only be rejected at most *K* times. Consequently, for each MUE, there exists an ℓ high enough such that in all rounds of the algorithm past ℓ, the MUE is assigned the same S-RRH, so the pointwise limit exists. To see that the limit is a matching, we only have to prove that the measure of MUEs assigned to each S-RRH is no more than its capacity. At the ℓ-th round of the algorithm, let R_ℓ be the measure of rejected MUEs. Again, because no MUE can be rejected more than *K* times, we have $R_\ell \to 0$. But at round ℓ, the number of MUEs assigned to each S-RRH has to be at most R_ℓ, so in the limit, each S-RRH is assigned at most its quota. Also, if the measure is less than the quota, then we know the S-RRH has not rejected any MUEs throughout the algorithm. ■

From the above propositions, we can see that the two-sided cooperator selection can acquire the unique and stable many-to-one matching solution. We also notice that the computational complexity increases when the number of MUEs and S-RRHs becomes larger. However, the computational complexity of the many-to-one stable matching depends on the total number of acceptable pairs [36]. The computational complexity of the proposed algorithm is $\mathcal{O}(M \times K)$, where *M* represents the number of MUEs and *K* denotes the number of S-RRHs, which is of low complexity and can be efficiently implemented in practice.

VI. Numerical Results

In this section, the proposed cooperation framework is evaluated via extensive simulations. The performance and interference level of MUEs and SUEs with and without cooperation are compared, respectively. Moreover, we illustrate how the values of α and P_k affect the cooperation utility, and the relationship between cooperation time fraction α and the transmission power of S-RRH P_k is also shown. In addition, the performance of the proposed two-sided cooperator selection algorithm is compared with the optimal solution.

We consider an H-CRAN with single hexagonal macrocell consisting of one macro-RRH, *K* S-RRHs, *M* MUEs and *N* SUEs. The SUEs are in coexistence with the MUEs on the same bandwidth 20 MHz. The macro RRH serves MUEs scheduled over *M* OFDMA subcarriers with equal bandwidth.

TABLE I
SIMULATION PARAMETER

Parameter	Value
Macro RRH coverage area	3 km
S-RRH coverage area	300 m
Number of users served by each S-RRH	10
Time slot duration	10 ms
System bandwidth	20 MHz
Maximum transmission power of S-RRH	46 dBm
Minimum transmission power of S-RRH	40 dBm
Transmission power of MUE	30 dBm
Transmission power of SUE with cooperation	30 dBm
Transmission power of SUE without cooperation	20 dBm
Path loss exponent	4
Log-normal shadow fading	1
Noise density	-174 dBm/Hz
Number of iterations	100

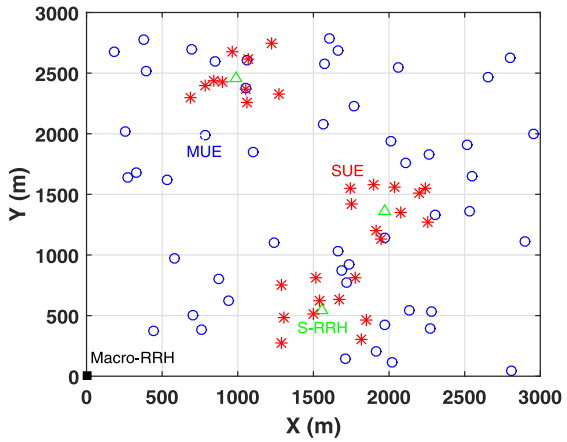

Fig. 3. H-CRAN deployment.

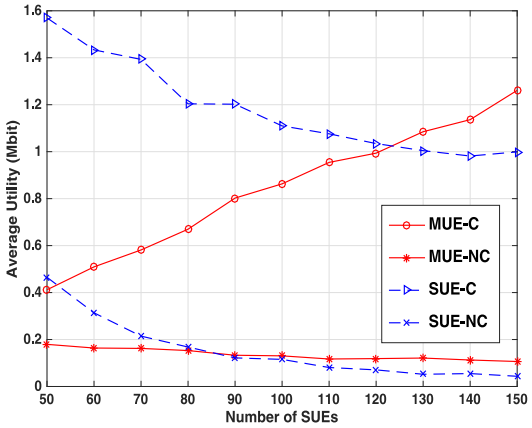

Fig. 4. Utility comparison with and without cooperation.

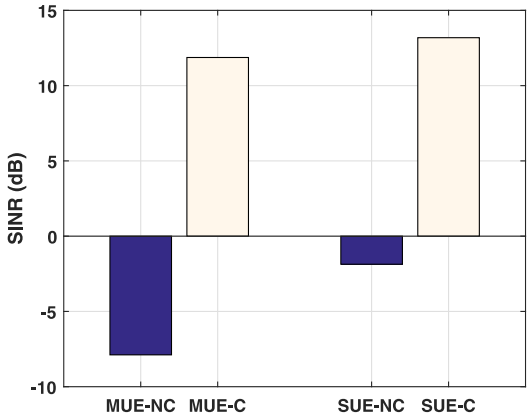

Fig. 5. Interference to MUE and SUE with and without cooperation.

Each S-RRH serves 10 SUEs which also use OFDMA spectrum access manner. A closed access policy is adopted at each S-RRH. The channel fading coefficients are obtained based on the deployment of RRHs and users, and they are calculated by $|h_{m,n}|^2 = d_{m,n}^{-\gamma}$, where $d_{m,n}$ is the distance from node m to n with a unit in meter and the path loss exponent γ is set to 4 [38]. The large scale fading is calculated based on path loss, while the small scale fading $|g|$ is the Rayleigh fading magnitude with $E[|g|^2] = 1$. The noise density is -174 dBm/Hz. Detailed simulation settings are summarized in Table I. The iteration in the simulation is used to obtain the average utility that accounts for the effect of randomness.

In Fig. 3, a simple H-CRAN scenario is illustrated. The M-RRH is represented by a solid square which is located at the origin. MUEs and S-RRHs are deployed uniformly on the 3000 $\times$ 3000 m^2 area. The S-RRHs are represented by the green triangles serving as the center of a disc of radius 300 m, in which SUEs are randomly located. Red stars denote the SUEs, and blue circles represent the MUEs. The number of MUEs and S-RRHs are 50 and 3, respectively. Each S-RRH serves 10 SUEs, and the number of SUEs is 30 accordingly.

As shown in Fig. 4, the number of S-RRHs varies from 5 to 15, and each S-RRH serves 10 SUEs. Accordingly, the number of SUEs varies from 50 to 150. The quota of the S-RRH is $q_k = 3$. The number of MUEs is 100. In our simulation, the preference ranking lists of the S-RRHs and MUEs are obtained according to the locations of the H-CRAN configuration. In Fig. 4, we compare the average utility of MUEs and SUEs with and without cooperation, respectively. The red line with circles represents the average utility of MUEs which cooperate with S-RRHs. The value increases as the number of S-RRHs becomes larger since the cooperators with better conditions are selected and more MUEs being involved in the cooperation. Moreover, it can be observed that the average utility obtained with cooperation outperforms that without cooperation. Not only the S-RRHs contribute to that by relaying transmission, but also the cooperation between S-RRHs and MUEs mitigates the interference to both small cell and macrocell networks.

In Fig. 5, the interferences to MUE and SUE (with and without cooperation) are illustrated, respectively. It is shown that the interference to both MUE and SUE are mitigated due to the cooperation between the S-RRH and MUEs. The reason for the interference mitigation of the SUE is that the cooperative MUEs stop the continuous retransmissions to the M-RRH since the S-RRH helps them relay their traffic to the M-RRH.

In Fig. 6, we show the relationship between cooperation time fraction α and the cooperation utility. We consider the M-RRH is located at the origin, and the MUE is located 1300 m far from the M-RRH. The x-axis represents the distance between the M-RRH and the S-RRH, and we vary the distance from 800 m to 1300 m. In this way, the S-RRH is

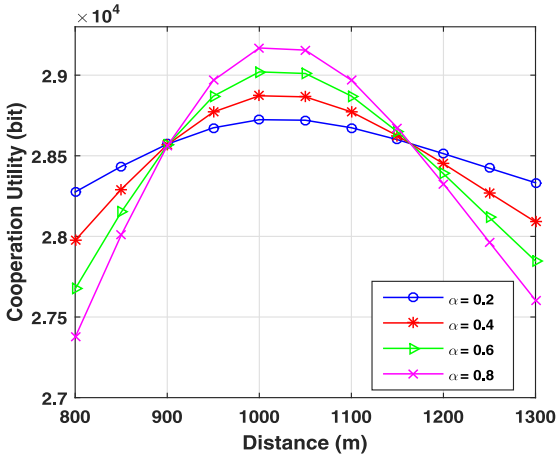

Fig. 6. Relationship between α and cooperation utility in different location scenarios.

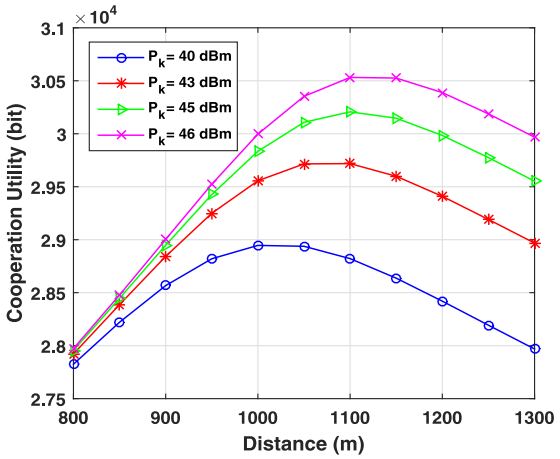

Fig. 7. Total utility as a function of α with different values of P_k.

moving from the macro RRH towards the MUE. We can see that the optimal value of $\alpha_{k,m}$ depends on the locations of the S-RRH between the M-RRH and the MUE. When the S-RRH is located in the middle between the M-RRH and the MUE, a larger α results in higher cooperation utility, and vice versa. A larger α results in higher cooperation utility since both the links from the S-RRH to the M-RRH and from the MUE to the S-RRH are good. Otherwise, when one of the links is in poor channel condition, a larger α will adversely affect the cooperation utility.

As shown in Fig. 7, as the value of P_k increases, the cooperation utility increases since higher transmission power leads to higher transmission rate. With different locations of S-RRH, the optimal solutions of P_k are different. Hence, we can conclude that the higher value of P_k contributes to higher cooperation utility which is consistent with the closed-form solution in (16).

In Fig. 8 and Fig. 9, we vary the cooperation time fraction α from 0.1 to 0.9, and vary the transmission power from the minimum to maximum. The utility of S-RRHs and MUEs and the total cooperation utility are shown. In Fig. 8, we can see that the utility of MUEs increases as the value of α becomes larger, while the utility of S-RRHs decreases. In

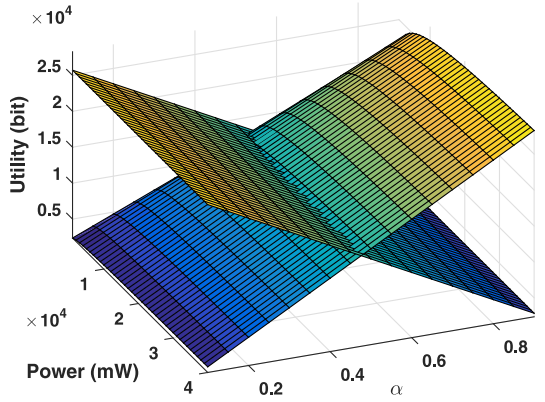

Fig. 8. The utility of S-RRHs and MUEs as a function of α and P_k.

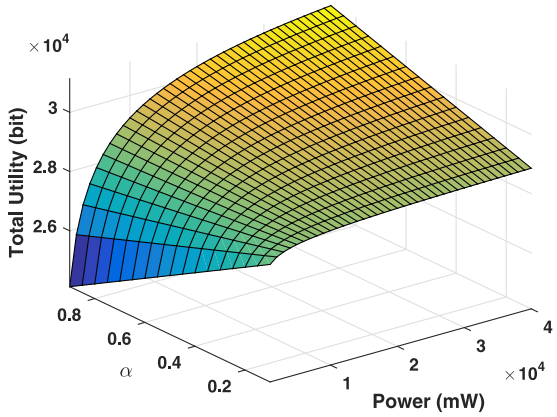

Fig. 9. Total cooperation utility as a function of α and P_k.

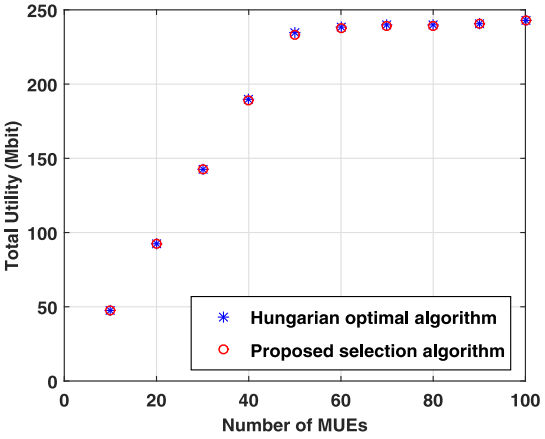

Fig. 10. Matching results comparison of the proposed algorithm and the optimal algorithm.

Fig. 9, it is shown that as the maximum total cooperation utility achieved at the maximum transmission power of S-RRH, and the optimal value of α depends on the locations of the M-RRH, S-RRHs and MUEs, since the locations of users affect the transmission channel conditions.

In addition, we also compare the total utility of our proposed two-sided cooperator selection algorithm with the Hungarian algorithm which gives the optimal solutions when $q_k = 1$. The number of S-RRHs is $K = 10$, and the number of MUEs

M varies from 10 to 100. As shown in Fig. 10, the blue stars represent the optimal results obtained by the Hungarian method, and the red circles are the results obtained by our proposed selection algorithm, which are very close to the optimal solutions.

VII. Concluding Remarks

In this paper, we have proposed a cooperation strategy for interference mitigation in H-CRAN. The cooperation problem is first formulated as a mixed integer programming, and is then transformed to a joint cooperation time and power allocation problem and a cooperator selection problem. We have solved the problems separately. Moreover, our proposed cooperator selection scheme takes both S-RRHs' and MUEs' utility into consideration. In addition, the inter-tier interference can be reduced. Simulation results have shown that the data transmission utility obtained by adopting our proposed two-sided cooperator selection approach can achieve near optimal performance in H-CRAN, and the cooperation can improve both the MUEs' and SUEs' utility compared with the non-cooperation solution. One of the applications of adopting our proposed cooperation framework is that the S-RRH can pre-cache popular contents to serve both MUEs and SUEs, which helps to reduce the traffic of fronthaul links. In the future work, we will investigate the clustered cooperation groups to further improve the network performance.

Appendix

Proof: Let $\xi_0 = (\alpha^*_{k,m}, P^*_k)$ be an optimal solution for any $k \in \mathcal{K}$ and $m \in \mathcal{M}$, we assume that the point is not at the boundary, which means that ξ_0 is within the region $1 - \frac{U^{min}_k}{TB_m G_{k,m}} \leq \alpha_{k,m} \leq 1$ and $P_{min} \leq P_k \leq P_{max}$. Then, the optimization problem $\mathcal{P}'_1$ can be rewritten as:

$$\begin{aligned}(\mathcal{P}''_1): \ &\text{minimize} \ \ f(\xi) \\ &\text{subject to} \ \ c_i(\xi) \geq 0, i \in \mathcal{I}\end{aligned} \tag{20}$$

where ξ_0 is defined as the feasible solution of problem $\mathcal{P}''_1$. Hence, $\mathcal{A}(\xi_0) = \{i \in \mathcal{I} : c_i(\xi) = 0\}$, where $c_i(\xi)$ are the constraints and ξ is the variable. The expression of $\mathcal{P}''_1$ is a more general and concise formulation which will ease the proof, and we need the following lemma for the proof.

Lemma (LICQ): Given the point and the active set, we say that the linear independence constraint qualification (LICQ) holds if the set of active constraint gradients is linearly independent [39].

In our case, within the feasible region $0 \leq \alpha_{k,m} \leq 1 - \frac{U^{min}_k}{TB_m G_{k,m}}$ and $P_{min} \leq P_k \leq P_{max}$ there is only one active set $c_i(\xi)$, which is $\alpha_{k,m} TB_m F_{k,m}(P_k) - U^{min}_m \geq 0$. Then, we have the gradient of $c_i(\xi)$ given by

$$\nabla c_i(\alpha_{k,m}, P_k) = \begin{pmatrix} TB_m F_{k,m}(P_k) \\ \frac{(1-c_0)(1-\alpha)c_3 \ln 2}{1+(1-\alpha)c_3 P_2} \end{pmatrix}. \tag{21}$$

Since, $\nabla c_i(\alpha_{k,m}, P_k)$ is not equal to 0, in other words, the set of $\mathcal{A}(\xi_0) = \{i \in \mathcal{I} : c_i(\xi) = 0\}$ is linearly independent. If LICQ holds at local solution ξ_0, Karush-Kuhn-Tucker (KKT) conditions must be satisfied. We have the Lagrangian function of optimization problem $\mathcal{P}''_1$ shown as

$$\begin{aligned}\mathcal{L}(\alpha_{k,m}, P_k, \lambda) &= f(\alpha_{k,m}, P_k) - \lambda g(\alpha_{k,m}, P_k) \\ &= TB_m\big\{\big[G_{k,m} - F_{k,m}(P_k)\big]\alpha_{k,m} - G_{k,m}\big\} \\ &\quad - \lambda\Big[\alpha_{k,m} TB_m F_{k,m}(P_k) - U^{min}_m\Big].\end{aligned} \tag{22}$$

The gradient of (22) is

$$\nabla c_i(\alpha_{k,m}, P_k) = \begin{pmatrix} \frac{\partial \mathcal{L}(\alpha_{k,m}, P_k, \lambda)}{\partial \alpha_{k,m}} \\ \frac{\partial \mathcal{L}(\alpha_{k,m}, P_k, \lambda)}{\partial P_k} \end{pmatrix} \tag{23}$$

where

$$\frac{\partial \mathcal{L}(\alpha_{k,m}, P_k, \lambda)}{\partial \alpha_{k,m}} = TB_m\big[\big(G_{k,m} - F_{k,m}(P_k)\big) - \lambda F_{k,m}(P_k)\big] \tag{24}$$

and

$$\frac{\partial \mathcal{L}(\alpha_{k,m}, P_k, \lambda)}{\partial P_k} = -TB_m \alpha D\big(1 + \alpha_{k,m}\big), \tag{25}$$

in which

$$\begin{aligned}D &= \frac{\partial P}{\partial F_{k,m}(P_k)} \\ &= \frac{h^4_{m,k} h^2_{k,0} P^2_m + h^2_{m,k} h^2_{k,0} P_m \sigma^2}{h^2_{m,k} P_m \sigma^2 + h^2_{k,0} P_k \sigma^2 + h^2_{m,k} h^2_{k,0} P_m P_k + \sigma^4} \\ &\quad \times \frac{\ln 2}{h^2_{m,k} P_m + h^2_{k,0} P_k + \sigma^2}.\end{aligned}$$

In reality, $\alpha_{k,m} = 0$ means the whole transmission time slot of the MUEs are given to the S-RRHs which is infeasible; $\alpha_{k,m} = 1$ means S-RRHs relay the data MUEs for the whole cooperation time slot, which is infeasible either, since S-RRH will not choose to cooperate with the MUE if there is no spectrum available that can be acquired as a reward for relaying. Since $\lambda_{k,m} \geq 0$, $T > 0$, $B > 0$ and $D > 0$, we can obtain that (23) does not equal to 0, which is in conflict with the KKT conditions. As mentioned above, we can see that the LICQ holds but the KKT conditions are not satisfied. Therefore, the assumption is not true and the optimal solution is on the boundary of the feasible set. From (11) and (12), we notice that the value of the objective function decreases when P_k becomes larger, so we have $P^*_k = P_{max}$. Then, the optimization problem becomes as follows:

$$\begin{aligned}&\underset{\alpha_{k,m}}{\text{minimize}} \ \ TB_m\big[G_{k,m} - F_{k,m}(P_{max})\alpha_{k,m} - G_{k,m}\big] \\ &\text{subject to} \ \ \alpha_{k,m} \geq \frac{U^{min}_m}{TB_m F_{k,m}(P_{max})} \\ &\qquad\qquad 0 < \alpha_{k,m} \leq 1 - \frac{U^{min}_k}{TB_m G_{k,m}}.\end{aligned} \tag{26}$$

Therefore, we can obtain the optimal solutions for three cases shown by (15) and (16). ■

REFERENCES

[1] Y. Tang, P. Yang, W. Wu, J. W. Mark, and X. S. Shen, "Cooperation-based interference mitigation in heterogeneous cloud radio access networks," in *Proc. IEEE Int. Conf. Commun. (ICC)*, Shanghai, China, May 2019, pp. 1–6.

[2] P. Yang, N. Zhang, Y. Bi, L. Yu, and X. S. Shen, "Catalyzing cloud-fog interoperation in 5G wireless networks: An SDN approach," *IEEE Netw.*, vol. 31, no. 5, pp. 14–20, Sep. 2017.

[3] M. Peng, X. Xie, Q. Hu, J. Zhang, and H. V. Poor, "Contract-based interference coordination in heterogeneous cloud radio access networks," *IEEE J. Sel. Areas Commun.*, vol. 33, no. 6, pp. 1140–1153, Jun. 2015.

[4] A. Checko *et al.*, "Cloud RAN for mobile networks: A technology overview," *IEEE Commun. Surveys Tuts.*, vol. 17, no. 1, pp. 405–426, 1st Quart., 2015.

[5] A. R. Dhaini, P.-H. Ho, G. Shen, and B. Shihada, "Energy efficiency in TDMA-based next-generation passive optical access networks," *IEEE/ACM Trans. Netw.*, vol. 22, no. 3, pp. 850–863, Jun. 2014.

[6] D. Zhang *et al.*, "Resource allocation for green cloud radio access networks with hybrid energy supplies," *IEEE Trans. Veh. Technol.*, vol. 67, no. 2, pp. 1684–1697, Feb. 2018.

[7] H. Zhang, C. Jiang, J. Cheng, and V. C. M. Leung, "Cooperative interference mitigation and handover management for heterogeneous cloud small cell networks," *IEEE Wireless Commun.*, vol. 22, no. 3, pp. 92–99, Jun. 2015.

[8] S.-M. Cheng, S.-Y. Lien, F.-S. Chu, and K.-C. Chen, "On exploiting cognitive radio to mitigate interference in macro/femto heterogeneous networks," *IEEE Wireless Commun.*, vol. 18, no. 3, pp. 40–47, Jun. 2011.

[9] Y. Tang, Q. Zhang, and W. Lin, "Artificial neural network based spectrum sensing method for cognitive radio," in *Proc. Int. Conf. Wireless Commun. Netw. Mobile Comput. (WiCOM)*, Chengdu, China, Sep. 2010, pp. 1483–1487.

[10] Q. Ye, W. Zhuang, S. Zhang, A.-L. Jin, X. Shen, and X. Li, "Dynamic radio resource slicing for a two-tier heterogeneous wireless network," *IEEE Trans. Veh. Technol.*, vol. 67, no. 10, pp. 9896–9910, Oct. 2018.

[11] A. Adhikary, H. S. Dhillon, and G. Caire, "Massive-MIMO meets HetNet: Interference coordination through spatial blanking," *IEEE J. Sel. Areas Commun.*, vol. 33, no. 6, pp. 1171–1186, Jun. 2015.

[12] C. Psomas, M. Mohammadi, I. Krikidis, and H. A. Suraweera, "Impact of directionality on interference mitigation in full-duplex cellular networks," *IEEE Trans. Wireless Commun.*, vol. 16, no. 1, pp. 487–502, Jan. 2017.

[13] X. Li, C. Li, S. Jin, and X. Gao, "Interference coordination for 3-D beamforming-based HetNet exploiting statistical channel-state information," *IEEE Trans. Wireless Commun.*, vol. 17, no. 10, pp. 6887–6900, Oct. 2018.

[14] T. K. Vu, M. Bennis, S. Samarakoon, M. Debbah, and M. Latva-Aho, "Joint load balancing and interference mitigation in 5G heterogeneous networks," *IEEE Trans. Wireless Commun.*, vol. 16, no. 9, pp. 6032–6046, Sep. 2017.

[15] J. Yoon, M. Y. Arslan, K. Sundaresan, S. V. Krishnamurthy, and S. Banerjee, "Self-organizing resource management framework in OFDMA femtocells," *IEEE Trans. Mobile Comput.*, vol. 14, no. 4, pp. 843–857, Apr. 2015.

[16] H. Zhang, C. Jiang, X. Mao, and H.-H. Chen, "Interference-limited resource optimization in cognitive femtocells with fairness and imperfect spectrum sensing," *IEEE Trans. Veh. Technol.*, vol. 65, no. 3, pp. 1761–1771, Mar. 2016.

[17] I. Budhiraja, S. Tyagi, S. Tanwar, N. Kumar, and M. Guizani, "Cross layer NOMA interference mitigation for femtocell users in 5G environment," *IEEE Trans. Veh. Technol.*, vol. 68, no. 5, pp. 4721–4733, May 2019.

[18] J. Chen, Y. Deng, J. Jia, M. Dohler, and A. Nallanathan, "Cross-layer QoE optimization for D2D communication in CR-enabled heterogeneous cellular networks," *IEEE Trans. Cogn. Commun. Netw.*, vol. 4, no. 4, pp. 719–734, Dec. 2018.

[19] A. Zaeemzadeh, M. Joneidi, N. Rahnavard, and G.-J. Qi, "Co-SpOT: Cooperative spectrum opportunity detection using Bayesian clustering in spectrum-heterogeneous cognitive radio networks," *IEEE Trans. Cogn. Commun. Netw.*, vol. 4, no. 2, pp. 206–219, Jun. 2018.

[20] C.-J. Liu and L. Xiao, "Interference precancellation for resource management in heterogeneous cellular networks," *IEEE Trans. Cogn. Commun. Netw.*, vol. 5, no. 1, pp. 138–152, Mar. 2019.

[21] F. Pantisano, M. Bennis, W. Saad, and M. Debbah, "Spectrum leasing as an incentive towards uplink macrocell and femtocell cooperation," *IEEE J. Sel. Areas Commun.*, vol. 30, no. 13, pp. 617–630, Apr. 2012.

[22] R. Urgaonkar and M. J. Neely, "Opportunistic cooperation in cognitive femtocell networks," *IEEE J. Sel. Areas Commun.*, vol. 30, no. 3, pp. 607–616, Apr. 2012.

[23] N. Zhang, H. Liang, N. Cheng, Y. Tang, J. W. Mark, and X. S. Shen, "Dynamic spectrum access in multi-channel cognitive radio networks," *IEEE J. Sel. Areas Commun.*, vol. 32, no. 11, pp. 2053–2064, Nov. 2014.

[24] B. Ma, M. H. Cheung, V. W. S. Wong, and J. Huang, "Hybrid overlay/underlay cognitive femtocell networks: A game theoretic approach," *IEEE Trans. Wireless Commun.*, vol. 14, no. 6, pp. 3259–3270, Jun. 2015.

[25] Y. Tang and J. W. Mark, "A quadrature signaling based cooperative scheme for cognitive radio networks," in *Proc. IEEE Glob. Commun. Conf. (GLOBECOM)*, Anaheim, CA, USA, Dec. 2012, pp. 1483–1487.

[26] R. Langar, S. Secci, R. Boutaba, and G. Pujolle, "An operations research game approach for resource and power allocation in cooperative femtocell networks," *IEEE Trans. Mobile Comput.*, vol. 14, no. 4, pp. 675–687, Apr. 2015.

[27] Y. Wu, J. Chen, L. Qian, J. Huang, and X. S. Shen, "Energy-aware cooperative traffic offloading via device-to-device cooperations: An analytical approach," *IEEE Trans. Mobile Comput.*, vol. 16, no. 1, pp. 97–114, Jan. 2017.

[28] W. Wu, N. Zhang, N. Cheng, Y. Tang, K. Aldubaikhy, and X. Shen, "Beef up mmWave dense cellular networks with D2D-assisted cooperative edge caching," *IEEE Trans. Veh. Technol.*, vol. 68, no. 4, pp. 3890–3904, Apr. 2019.

[29] P. Xia, V. Chandrasekhar, and J. Andrews, "Open vs. closed access femtocells in the uplink," *IEEE Trans. Wireless Commun.*, vol. 9, no. 12, pp. 3798–3809, Dec. 2010.

[30] M. Latham, "Consumer attitudes to femtocell enabled in-home services-insights from a European survey," in *Proc. Femtocells Europe*, Jun. 2008.

[31] A. Masmoudi and T. Le-Ngoc, "Channel estimation and self-interference cancelation in full-duplex communication systems," *IEEE Trans. Veh. Technol.*, vol. 66, no. 1, pp. 321–334, Jan. 2017.

[32] A. Nosratinia and T. E. Hunter, "Grouping and partner selection in cooperative wireless networks," *IEEE J. Sel. Areas Commun.*, vol. 25, no. 2, pp. 369–378, Feb. 2007.

[33] C. L. He, B. Sheng, P. C. Zhu, X. H. You, and G. Y. Li, "Energy- and spectral-efficiency tradeoff for distributed antenna systems with proportional fairness," *IEEE J. Sel. Areas Commun.*, vol. 31, no. 5, pp. 894–902, May 2013.

[34] J. N. Laneman, D. N. C. Tse, and G. W. Wornell, "Cooperative diversity in wireless networks: Efficient protocols and outage behavior," *IEEE Trans. Inf. Theory*, vol. 50, no. 12, pp. 3062–3080, Dec. 2004.

[35] D. Gale and L. S. Shapley, "College admissions and the stability of marriage," *Amer. Math. Month.*, vol. 69, no. 1, pp. 9–15, Jan. 1962.

[36] Y. Gu, W. Saad, M. Bennis, M. Debbah, and Z. Han, "Matching theory for future wireless networks: Fundamentals and applications," *IEEE Commun. Mag.*, vol. 53, no. 5, pp. 52–59, May 2015.

[37] D. F. Manlove, *Algorithmics of Matching Under Preferences*. Hackensack, NJ, USA: World Sci., Apr. 2013.

[38] S. Zhang, P. He, K. Suto, P. Yang, L. Zhao, and X. Shen, "Cooperative edge caching in user-centric clustered mobile networks," *IEEE Trans. Mobile Comput.*, vol. 17, no. 8, pp. 1791–1805, Aug. 2018.

[39] J. Nocedal and S. J. Wright, *Numerical Optimization*, 2nd ed. New York, NY, USA: Springer, 2006.

Yujie Tang (S'12–M'19) received the B.E. degree in communications engineering from Lanzhou Jiaotong University, Lanzhou, China, the M.Sc. degree in information and communications engineering from the Harbin Institute of Technology, Harbin, China, and the Ph.D. degree in electrical and computer engineering from the University of Waterloo, Waterloo, ON, Canada. Then, she was a Post-Doctoral Fellow with the Broadband Communications Research Group, University of Waterloo. She is currently an Assistant Professor with the Department of Computer Science and Mathematics, Algoma University, Sault Ste. Marie, ON, Canada. Her research interests include Internet of Vehicles, software-defined networks, machine learning, cognitive radio networks, cooperative networks, and resource management in heterogeneous networks.

Peng Yang (S'16–M'18) received the B.E. degree in communication engineering from the School of Electronic Information and Communications, Huazhong University of Science and Technology, Wuhan, China, in 2013, and the Ph.D. degree in information and communication engineering from the Huazhong University of Science and Technology in 2018. Since September 2018, he has been working as a Post-Doctoral Fellow with the Broadband Communications Research Group, Department of Electrical and Computer Engineering, University of Waterloo, Canada, where he was a visiting Ph.D. student from September 2015 to September 2017. His current research focuses on software-defined networking, mobile edge computing, and video streaming.

Wen Wu (S'13) received the B.E. degree in information engineering from the South China University of Technology, Guangzhou, China, and the M.E. degree in electrical engineering from the University of Science and Technology of China, Hefei, China, in 2012 and 2015, respectively, and the Ph.D. degree in electrical and computer engineering from the University of Waterloo, Waterloo, ON, Canada, in 2019. Since 2019, he has been working as a Post-Doctoral Fellow with the Department of Electrical and Computer Engineering, University of Waterloo. His research interests include millimeter-wave networks and AI-empowered wireless networks.

Jon W. Mark (M'62–SM'80–F'88–LF'03) received the B.A.Sc. degree in electrical engineering from the University of Toronto in 1962, and the M.Eng. and Ph.D. degrees in electrical engineering from McMaster University, Canada, in 1968 and 1970, respectively.

From 1962 to 1970, he was an Engineer and then a Senior Engineer with Westinghouse Canada Ltd., where he conducted research in advanced sonar signal processing. From 1968 to 1970, he was on leave from Westinghouse to pursue Ph.D. studies at McMaster University under the auspices of an NRC PIER Fellowship. In September 1970, he joined the Department of Electrical Engineering, University of Waterloo, where he was promoted to the rank of Full Professor in July 1978 and served as the Department Chairman from July 1984 to June 1990. During this period, the department introduced the computer engineering degree program and changed the name to Electrical and Computer Engineering. He was on sabbatical leaves with the IBM Thomas J. Watson Research Center, Yorktown Heights, NY, USA, as a Visiting Research Scientist from 1976 to 1977; with Bell Labs, Murray Hill, NJ, USA, as a Resident Consultant from 1983 to 1984, with the Université Pierre et Marie Curie, Paris, France, as an Invited Professor from 1990 to 1991, and the National University of Singapore as a Visiting Professor from 1994 to 1995. In 1996, he established the Centre for Wireless Communications (CWC) with the University of Waterloo, with a $1 million donation from Ericsson Canada as seed money. He is currently a Distinguished Professor Emeritus and the Founding Director of CWC with the University of Waterloo. He has coauthored the book entitled *Wireless Communications and Networking* (Prentice-Hall, 2003), *Multimedia Services in Wireless Internet* (Wiley, 2009), and *Wireless Broadband Networks* (Wiley, 2009). His current research interests are in wireless communications and interdomain networking, with a focus on cooperative networking, cognitive radio networking, power control, and resource allocation.

Dr. Mark received the 2000 Canadian Award in Telecommunications Research for significant research contributions, scholarship and leadership in the fields of computer communication networks and wireless communications and the 2000 Award of Merit by the Education Foundation of the Association of Chinese Canadian Professionals for Significant Contributions in Telecommunications Research. He is a fellow of the Canadian academy of Engineering. He has served as a member of a number of editorial boards, including editorships in the IEEE TRANSACTIONS ON COMMUNICATIONS, *Wireless Networks*, and *Telecommunication Systems*, a member of the Inter-Society Steering Committee of the IEEE/ACM Transactions on Networking from 1992 to 2003 (as the SC Chair from 1999 to 2000), and a member of the IEEE Communications Society Awards Committee from 1995 to 1998.

Xuemin (Sherman) Shen (M'97–SM'02–F'09) received the Ph.D. degree in electrical engineering from Rutgers University, New Brunswick, NJ, USA, in 1990.

He is currently a University Professor with the Department of Electrical and Computer Engineering, University of Waterloo, Canada. His research focuses on resource management, wireless network security, social networks, 5G and beyond, and vehicular ad hoc and sensor networks. He is an Engineering Institute of Canada Fellow, a Canadian Academy of Engineering Fellow, a Royal Society of Canada Fellow, a Chinese Academy of Engineering Foreign Fellow, a registered Professional Engineer of Ontario, Canada, and a Distinguished Lecturer of the IEEE Vehicular Technology Society and Communications Society. He received the R.A. Fessenden Award in 2019 from IEEE, Canada, Award of Merit by the Education Foundation of the Association of Chinese Canadian Professionals in 2019, the James Evans Avant Garde Award in 2018 from the IEEE Vehicular Technology Society, the Joseph LoCicero Award in 2015 and Education Award in 2017 from the IEEE Communications Society, the Excellent Graduate Supervision Award in 2006 and Outstanding Performance Award 5 times from the University of Waterloo and the Premier's Research Excellence Award in 2003 from the Province of Ontario. He served as the Technical Program Committee Chair/Co-Chair for the IEEE Globecom'16, the IEEE Infocom'14, the IEEE VTC'10 Fall, the IEEE Globecom'07, the Symposia Chair for the IEEE ICC'10, the Tutorial Chair for the IEEE VTC'11 Spring, and the Chair for the IEEE Communications Society Technical Committee on Wireless Communications. He is the Editor-in-Chief of the IEEE INTERNET OF THINGS JOURNAL and the Vice President on Publications of the IEEE Communications Society.